Three-dimensional Simulations of Passively Autonomous Load-follow Operation

Ahmed Amin E. Abdelhameed, Seongdong Jang and Yonghee Kim*
Department of Nuclear & Quantum Engineering
Korea Advanced Institute of Science and Technology
291 Daehak-ro Yuseong-gu, Daejeon, Korea, 34141
**Corresponding author: yongheekim@kaist.ac.kr*

1. Introduction

In the passively autonomous load-follow operation (PLFO), the core coolant temperature variation is used to perturb the reactor and compensate for the reactivity feedback from Xe and fuel during power maneuvering without any active reactivity control. For, a soluble-boron-free (SBF) small modular reactor (SMR), there is two reasons that can allow utilizing this new operational scheme. First, due to absence of boron in the coolant system, coolant temperature coefficient (CTC) is strongly negative, even at the beginning of cycle, which means a relatively small change in coolant temperature is effective in perturbing the core reactivity. Second, in SMRs the power density is typically smaller than that of big-size pressurized water reactors (PWRs), which yields less Xe reactivity feedback [1, 2]. The objective of this paper is to demonstrate numerical results of PLFO in a 450MWth small SBF PWR, using a three-dimensional transient and thermal-hydraulic (TH) coupled nodal algorithm that is solved using an in-house FORTRAN code. The various cross-sections and transient parameters are obtained using Monte Carlo simulations using Serpent-2 code with ENDF/B-VII7.1 data library.

2. Methods and Results

PLFO scheme is investigated for a SBF small PWR called "ATOM", which stands for autonomous transportable on-demand reactor module. The major technical parameters of ATOM are shown in Table. I. ATOM core utilizes 12 mechanical shim (MS) banks, 12 regulating banks, and 25 shutdown banks [3]. The neutronic solution is obtained using 3-D nodal expansion method (NEM) algorithm. The starting point of the numerical simulation is achieving a critical steady-state core condition at hot full power by the mechanical shim (MS) adjustment. In the radial direction, 1 node per fuel assembly discretization is used with implementing the assembly discontinuity factor (ADF) in the fuel region. In the axial direction, 24 axial nodes are considered. The TH module is based on core analyses for each of the 69 fuel channels in the ATOM core. The TH solutions is obtained by the field flow module, that consists of solving the axial momentum balance, mass balance and energy balance equations, and by solving the heat conduction for each discretized node. Similarly to the neutronic module, 24 axial nodes are considered for each fuel channel. Detailed descriptions of the neutronic and TH modules are given in Sections 2.1 and 2.2.

Table I: Major technical parameters of ATOM core.

Parameter	Value
Reactor Power	
Reactor Power (MWt)	450
Specific power (W/gU)	25.99
Core Dimensions	
Active core height (cm)	200
Equivalent diameter (cm)	201.6
Height-to-diameter ratio	0.993
Core Description	
Number of fuel assemblies (FAs)	69
FA array	17 x 17
Fuel materials	UO2
Fuel Management	
Fuel loading	Single-batch
Cycle length (months)	> 48
Fuel Assembly	
Fuel assembly design	17 x 17
Number of fuel rod	264
Number of guide thimbles	24
Number of central tube	1
Pitch-to diameter ratio (P/D)	1.326
Assembly pitch (cm)	21.503
Pin pitch (cm)	1.259
Fuel enrichment (w/o)	5

2.1 Neutronic algorithm

The neutronic algorithm is based on NEM. It starts by taking initial guesses of the multiplication factor (K_{eff}), node average flux, incoming partial currents on the right and left surfaces for x, y and z directions. The transverse leakage expansion coefficients are then updated. The low order flux coefficients are updated using the surface fluxes. The high order coefficients are calculated in terms of the low order coefficients and transverse leakage coefficients using the weighted residual method. The next step is to obtain the node average flux in terms of the incoming partial currents and high order flux coefficients, as given in Eq. 1. Then, the outgoing partial currents from the node surfaces to the neighboring nodes in x, y and z directions are

calculated in terms of the incoming partial currents and node average flux. Node and group sweeps are performed. The power method iterations are used to obtain a converged power source and K_{eff}.

$$\overline{\Phi_g^{\varpi}} = \frac{1}{\Sigma_{rg}^{\varpi} + \sum_{u=x,y,z} \frac{1}{\Delta u}(C_{0gul} + C_{0gur})} \left(\sum_{g'=1}^{G} [\Sigma_{sg'g}^{\varpi} + (1-\beta)\frac{X_{gp}}{K} \nu \Sigma_{fg}^{\varpi}] \overline{\Phi_{g'}^{\varpi}} - \frac{1}{v_g}\frac{\partial}{\partial t}\overline{\Phi_g^{\varpi}} \right.$$
$$+ \sum_{i=1}^{I} X_{dgi}\lambda_i C_i + \sum_{u=x,y,z} \frac{1}{\Delta u}(J_{gur}^{-\varpi}(1 - C_{1gur} - C_{2gul}) + J_{gul}^{+\varpi}(1 - C_{2gur} - C_{1gul}) \quad (1)$$
$$\left. - a_{3gu}(C_{3gul} - C_{3gur}) + a_{4gu}(C_{4gul} + C_{4gur}))\right)$$

As shown in Fig.1, after the convergence of the neutronic module, the thermal hydraulic (TH) are carried out. This is followed by updating the XSs by taking into account the temperature deviations and the concentrations of Xe-135 and SM-149, as shown in Eqs. 2-3. Iterations are required to obtain a converged static TH-coupled nodal solution.

$$\Sigma(T_f, T_m, \mathrm{D}_m, \mathrm{Sb}) = \Sigma_r + \frac{\partial \Sigma}{\partial T_f}\Delta\sqrt{T_f} + \frac{\partial \Sigma}{\partial T_m}\Delta T_m + \frac{\partial \Sigma}{\partial \mathrm{D}_m}\Delta \mathrm{D}_m \quad (2)$$
$$+ \frac{\partial \Sigma}{\partial Sb}\Delta Sb + \frac{\partial^2 \Sigma}{2\partial \mathrm{D}_m^{\,2}}(\Delta \mathrm{D}_m)^2$$

$$\Sigma_{a,g} = \Sigma_{a,g} + \Delta\Sigma_{\mathrm{Xe,a},g} + \Delta\Sigma_{Sm,\mathrm{a},g} \quad (3)$$

The transient problem is solved as a fixed source problem. The solution of fixed source NEM is obtained and coupled with time-dependent TH modules to update the XSs and to obtain a converged TH-coupled transient solution. Then, the concentrations of delayed neutrons precursors are updated by Eq.4. In addition, the concentrations of the transient Xe-135 and Sm-149 are updated by solving the forward differences of the decay chains of I -135, Xe-135, Pm-149 and Sm-149.Besides the output current, the MATLAB detector code calculates the detector capacitance. The calculated output current is the input for the rest of the detector channel and the detector capacitance is an important input parameter.

$$C_i(t_c) = C_i(t_p)\mathrm{q}_{1,i} + \frac{X_{i,g}\beta_i F\phi_g(t_p)}{K_0} q_{2,i} + \frac{X_{i,g}\beta_i F\phi_g(t_c)}{K_0} q_{3,i} \quad (4)$$

$$q_{1,i} = e^{-\lambda_i \Delta t},$$

$$q_{2,i} = \frac{1 - e^{-\lambda_i \Delta t} - \lambda_i \Delta t_s e^{-\lambda_i \Delta t}}{\lambda_i^{\,2} \Delta t_s},$$

$$q_{3,i} = \frac{e^{-\lambda_i \Delta t}\left(1 - e^{\lambda_i \Delta t} + \lambda_i \Delta t_s e^{\lambda_i \Delta t}\right)}{\lambda_i^{\,2} \Delta t}$$

2.2 Thermal-hydraulic algorithm

The TH module performs core analysis by doing calculation for all fuel channels in the core. This is done by knowing the axial power distribution in each channel, from the 3-D dynamic neutronic module, and the core inlet coolant temperature based on the requested power demand. In order to calculate coolant temperature, the pressure drop (ΔP), which satisfies the mass balance equation is found, by solving the axial momentum balance equation and updating flow velocity (v) and ΔP until the mass balance is satisfied. Then, the energy balance equation is solved until a converged enthalpy (h) and coolant temperature values are obtained. Mass, axial momentum and energy balance equations are given in Eqs. 5, 6 and 7. No consideration of the lateral momentum was made in the current version of the code. For each axial node, the fuel heat transfer module solves the heat conduction equation in the radial direction for discretized nodes using finite-difference method, as shown in Eq. 8. It is well-known that as power demand varies the steam governor and the feed-water control valves are utilized to deliver the requested power demand while maintaining pressure of the secondary at the programmed value as demonstrated in Fig. 2. This yields variation of the amount of heat transferred from primary side loop to the secondary loop of the PWR, which changes the inlet coolant temperature to the core. In this paper, we simulate the variation of the heat transferred from primary loop to the secondary one using simple lumped steam generator (SG) model, Eq.9.

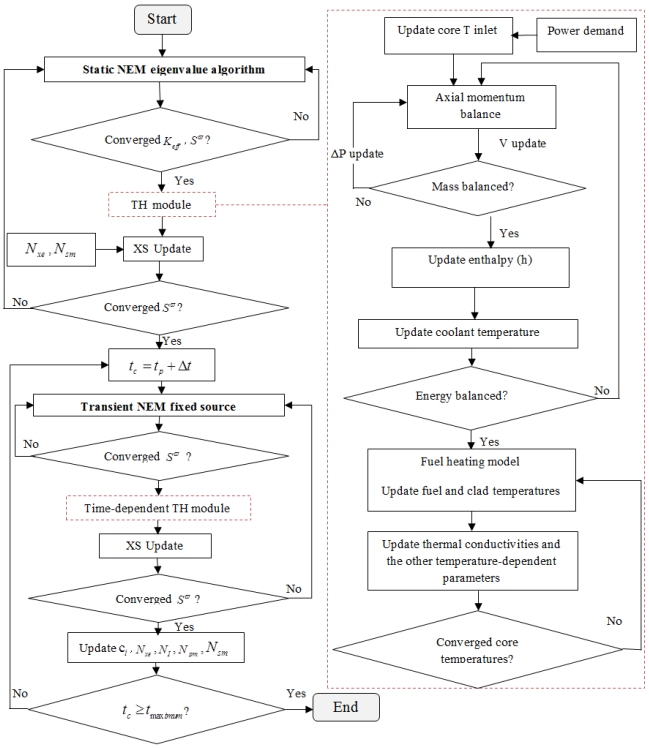

Fig. 1. Algorithm flowchart

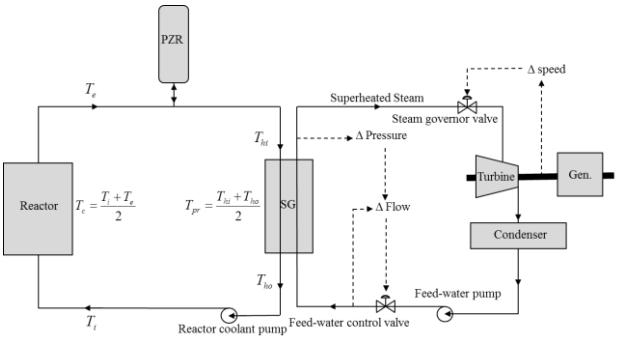

Fig. 2. Simplified PWR system diagram.

$$\Delta m_i = \Delta z A_i \frac{\partial \rho_i}{\partial t} - \Delta z \sum_{j=1}^{J} W_{ij} \tag{5}$$

$$\Delta(m_i v_i) = -\Delta z \frac{\partial m_i}{\partial t} - A_i \Delta P_i - A_i \rho_i g \Delta z - F_i - \Delta z \sum_{j=1}^{J} W_{ij}^{*}(v_i - v_j) - \sum_{j=1}^{J} W_{ij}^{*}(v^{*}) \tag{6}$$

$$\frac{\Delta(m_i h_i)}{\Delta z} = -A_i \frac{\partial(\rho_i h_i)}{\partial t} + q_i^{'} - \sum_{j=1}^{J} W_{ij}\, h_{ij}^{*} - (\sum_{j=1}^{J} W_{ij}^{*}(h_i - h_j) - \sum_{j=1}^{J} \overline{K}_c \frac{s_{ij}(T_i - T_j)}{l_{ij}}) \tag{7}$$

$$\rho_j C_{p,j} V_j \frac{\partial T_j}{\partial t} = Q_j^{''} V_j + Q_{j-1,j} + Q_{j+1,j} \tag{8}$$

$$M_{sg} c_c \frac{\partial T_{pr}}{\partial t} = w c_c [T_{hi} - T_{ho}] - h_{sg} A_{sg} \Gamma [T_{pr} - T_{sg}] \tag{9}$$

2.3 3-D PLFO Simulations

The studied scenario here is a load-follow scenario 100-50-100 with power ramping rate of 5% per minute, which is the maximum requested power ramping speed for load-follow[4]. The study is made for the ATOM core at middle of cycle (MOC) fuel condition. Figure 3 shows the reactor passive response plotted together with power demand. As power demand decrease less heat is transferred to the secondary side and the inlet coolant temperature increases, as shown in Fig.4, therefore the reactor power starts to decrease due to the negative coolant reactivity.

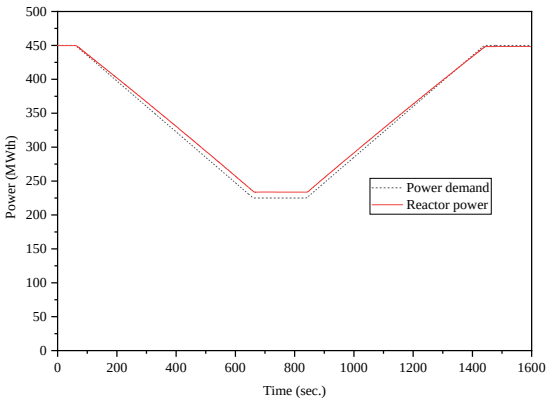

Fig. 3. Reactor power and power demand variations during 100-50-100 PLFO.

In addition, the decrease in the core power leads to increasing Xe and Sm concentrations which means a negative reactivity response from Xe and Sm. Moreover, The decrease of fuel temperature produces positive reactivity feedback due to the negative fuel temperature coefficient in the core (FTC), it is about -2.65 pcm/K at MOC in ATOM.

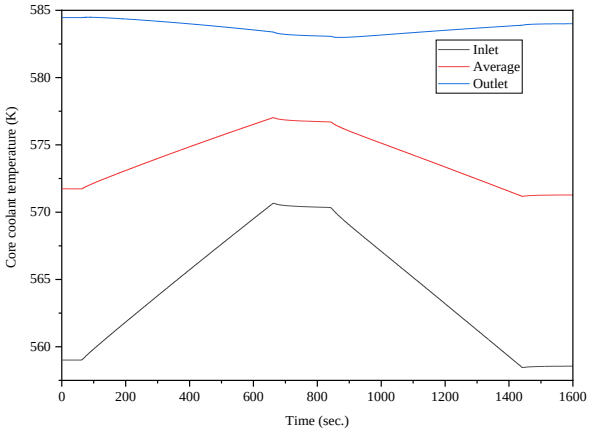

Fig. 4. Core coolant temperatures variations during 100-50-100 PLFO.

Because of the strongly negative CTC value of about -52pcm/K, largely negative coolant reactivity feedback is generated leading to decreasing the reactor power to follow the power demand variation without any control rod movement in the SBF core. About 5K deviation of the core average coolant transient is noticed during the 100-50-100 PLFO transients. Figure 5 shows the variation of the effective fuel temperature averaged over the various core channels. Axial shape index (ASI) variation during the PLFO transients is shown in Fig. 6. The maximum ASI deviation noticed is about -0.05 asiu. The axial power density variation with time during the PLFO transients is given in Fig. 7. It is clear that at 50% power level the axial shape is the least bottom skewed due to the increase in inlet coolant temperature with power decrease in the PLFO.

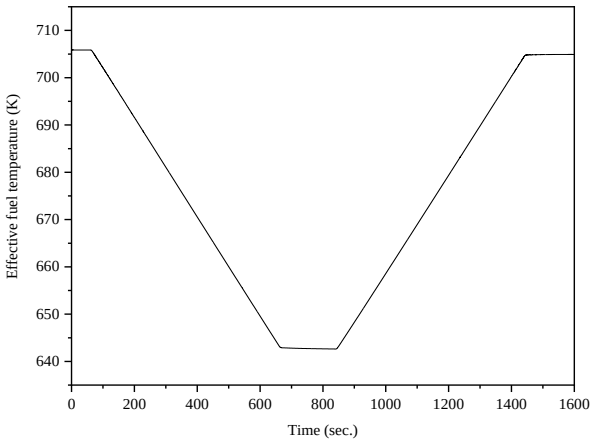

Fig. 5. Average effective fuel temperature variation during 100-50-100 PLFO.

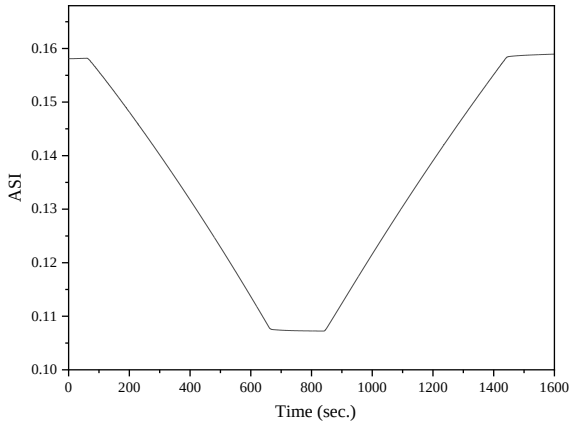

Fig. 6 . Deviation of the axial shape index during 100-50-100 PLFO.

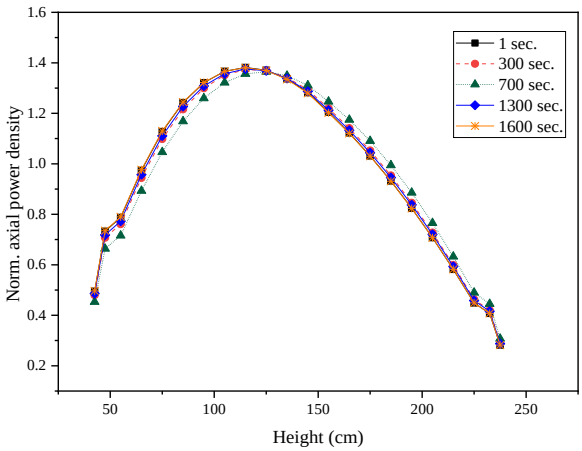

Fig. 7 Variation of the normalized axial power density distribution with time during the 100-50-100 PLFO.

3. Conclusions

3-D nodal simulations of the passively autonomous load-follow control operation are made for the 450MWth SBF ATOM SMR. 100-50-100 load-follow scenario is investigated. Typical maximum power ramping speed for load-follow is used in the simulation, 5% per minute. In the passively autonomous operation no active control by mechanical or chemical shims are utilized during the load-follow operation. Limited variation of the average coolant temperature and ASI are noticed in the SBF ATOM SMR core during the 100-50-100 PLFO. Further researches are currently on-going for investigating various load-follow scenarios and to improve the modeling of the various system components.

ACKNOWLEDGEMENTS

The National Research Foundation of Korea Grant funded by the Korean Government (MSIP) (NRF-2016R1A5A1013919) supported this work.

REFERENCES

[1] Abdelhameed, A.A.E., J. Lee, and Y. Kim, Physics conditions of passive autonomous frequency control operation in conventional large-size PWRs. Progress in Nuclear Energy, 2020. 118: p. 103072..

[2] Abdelhameed, A.A.E., et al., Feasibility of passive autonomous frequency control operation in a Soluble-Boron-Free small PWR. Annals of Nuclear Energy, 2018. 116: p. 319-333.

[3] Nguyen, X.H., C. Kim, and Y. Kim, An advanced core design for a soluble-boron-free small modular reactor ATOM with centrally-shielded burnable absorber. Nuclear Engineering and Technology, 2019. 51(2): p. 369-376.

[4] Lokhov, A., Technical and economic aspects of load following with nuclear power plants. NEA, OECD, Paris, France, 2011.